Photochemistry of "Super"-Photoacids. Solvent Effects

Kyril M. Solntsev[†] **and Dan Huppert**

School of Chemistry, Raymond and Beverly Sackler Faculty of Exact Sciences, Tel-Aviv University, Tel Aviv 69978, Israel

Noam Agmon*

The Fritz Haber Research Center, Department of Physical Chemistry, The Hebrew University, Jerusalem 91904, Israel

Received: January 19, 1999; In Final Form: May 11, 1999

We study steady-state and time-resolved fluorescence of 5-cyano-2-naphthol in various pure solvents. To some of these, excited-state proton transfer occurs within the excited-state lifetime of the chromophore. Solvatochromic shifts in the acid and anion bands are analyzed using the empirical Kamlet−Taft approach. The hydrogen-bond donated from the OH group to basic solvents accounts for most of the shift in the excitation spectra. This bond produces considerably larger shifts in the emission spectra, suggesting that it strengthens in the excited state. In contrast, the hydrogen bond donated from protic solvents to the hydroxyl oxygen is cleaved following photoexcitation. This bond (and not the change in dielectric constant) is responsible for the solvent-induced blue shift in anion fluorescence. Hence it must re-form simultaneously with the proton-transfer event. Our time-resolved fluorescence data fit the solution of the Debye−Smoluchowski equation for reversible geminate recombination in a field of force, provided that the difference in excited-state lifetimes and contact quenching are taken into account. An extended theory of reversible geminate recombination provides an accurate description of the asymptotic behavior in this case. The quenching processes correlate with the solvent hydrogen-bond donation ability, implicating the involvement of hydrogen-bonded pathways.

I. Introduction

Hydroxyarenes (ROH compounds) and aminoarenes (RNH_2 compounds) undergo significant enhancement in their acidity upon electronic excitation.[1−3] Hence molecules of this type are widely used as excited-state acid−base fluorescence probes in homogeneous solutions and microheterogeneous systems.[4] For example, the acidity of 2-naphthol (2OH) in water increases from $pK_a = 9.5$ in the ground state (S_0) to $pK_a^* = 2.8$ in its excited state (S_1).[1] It can transfer proton to water during its excited-state lifetime (ca. 8 ns), in a protolytic photodissociation process known as excited-state proton transfer to solvent (PTTS). However, the range of most solvents investigated was limited to water and its mixtures with various organic cosolvents, where acidity of photoacids was sufficient to observe photodissociation during their radiative lifetimes. Only a few examples of PTTS in nonaqueous solvents are known. For example, photodissociation of aminoaromatic cations ($ArNR_2H^+$) has been investigated in alcohols[5,6] and nitriles.[7,8] This requires preliminary ground-state protonation with strong acids, so that the elementary geminate PTTS event could not be probed. For hydroxyaromatics, two reports of PTTS in nonaqueous media involve *N*-methylsalicylamide in alcohols,[9] and 4-methyl-2,6-diformylphenol in dimethyl sulfoxide (DMSO), dimethylformamide (DMFA), and alcohols.[10,11]

Recently, enhanced photoacids based on mono- and dicyano derivatives of 2OH have been synthesized and characterized.[12,13] Preliminary investigations have shown that hydroxyaromatic compounds with electron-withdrawing cyano substituents dramatically increase their excited-state acidity as compared to parent molecules.[12−14] For example, 5-cyano-2-naphthol (5CN2OH) has $pK_a^* \approx -1$. The nearly 4 pK_a unit difference from 2OH is sufficient to allow proton transfer also to solvents less polar than water (alcohols, DMSO). Thus a systematic investigation of solvent effects on these reactions becomes feasible. The present work extends our previous reports concerning the steady-state[15] and time-resolved[14] fluorescence of 5CN2OH in various solvents.

The extremely high photoacidity of cyanonaphthols results in large solvatochromic shifts, as revealed by their steady-state fluorescence spectra. Our preliminary investigation of the solvatochromism of 5CN2OH demonstrated the dominant role of specific solvation.[15] Stabilization by a single hydrogen bond (HB), between the photolabile hydroxylic hydrogen and proton-accepting solvents, has a magnitude similar to that of nonspecific polar solvation. A Kamlet−Taft analysis[16,17] of the emission spectra revealed that this HB strengthens considerably upon excitation. In the present work, we investigate in more detail the solvatochromism in both emission and excitation spectra of 5CN2OH.

The mechanism of PTTS from cyanonaphthols in homogeneous alcoholic and aqueous solutions has been investigated by picosecond time-resolved measurements.[14,18,19] It may be depicted schematically by the following scheme

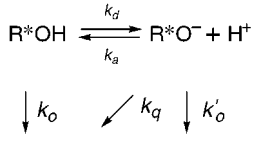

[†] Also in the Department of Physical Chemistry, The Hebrew University, Jerusalem 91904, Israel.

10.1021/jp9902295 CCC: $18.00
Published on Web 08/13/1999

In this mechanism, the initial state is that of a vibrationally relaxed, electronically excited ROH molecule (denoted by R*OH). It may dissociate to produce a "contact" geminate pair with a rate coefficient k_d. This pair may either separate by diffusion or recombine adiabatically, with an association rate coefficient k_a, to regenerate the initial state. A nonadiabatic process, which competes with proton recombination, is quenching by the geminate proton,[13,20−22] characterized by the rate coefficient k_q. In contrast to nonsubstituted naphthols, where proton-induced fluorescence quenching is usually attributed to aromatic ring protonation,[20] in cyanonaphthols this process might be initiated by a proton attack on the cyano nitrogen atom.[13] Finally, k_0 and k_0' are the reciprocal excited-state lifetimes of the bound and unbound states, respectively. Typically, the base lives longer than the acid, so that $k_0' < k_0$.

We have demonstrated in the past that an accurate determination of the various rate coefficients cannot rely on kinetic rate equations, which ignore the relative diffusional motion of the excited-anion and solvated proton.[23−25] Quantitative analysis requires the solution of the transient Debye−Smoluchowski equation (DSE) for describing the diffusional effects. It allows us to use the information in the nonexponential fluorescence decay tails for determining the association rate coefficient, k_a. A previous report[14] has applied this approach for PTTS from 5CN2OH to water and methanol. It will be extended below to additional solvents. However, the quenching process, which is required for a realistic description of cyanonaphthol kinetics in protic solvents,[13] has been ignored. The more complete analysis detailed below will consider all the rate processes depicted in the above reaction scheme. It is only recently that the effect of different lifetimes and quenching has been considered theoretically.[26−29] Useful approximate expressions for the binding and survival probabilities have been derived, as well as their exact long-time asymptotic behavior. These theoretical results will be compared with our data for PTTS from 5CN2OH to various pure solvents.

The comparison of experiment and theory provides a reasonably reliable set of kinetic parameters for the various solvents. This will allow us to address the question of solvent effects on excited-state PTTS kinetics. Previous studies suggest that, with an increase of the acidity in the series of monocyanonaphthol isomers, k_d increases and its isotope effect decreases.[14,19] This is in line with structure−reactivity correlations applied to proton-transfer reactions.[30−34] The upper limit for k_d may reflect the required solvent organization time. A study of the temperature effect on 5,8-dicyano-2-naphthol dissociation in alcohols[18] revealed that the activation energy for k_d is not constant. At low temperatures it is about the same as the activation energy for dielectric relaxation, but it becomes considerably smaller at elevated temperatures. While we do not report on temperature effects in the present study, the methods described below will enable us to investigate solvent effects not only on k_d but also on the recombination and quenching rate parameters.

II. Experimental Section

A. Materials. 5CN2OH was synthesized by Tolbert and coworkers as previously described.[12,13] Its methoxy derivative, 5-cyano-2-methoxynaphthalene (5CN2OMe), is the precursor along the synthetic route and thus readily available. The methanol solvent was BDH HPLC grade with <0.05% water without further treatment. Sodium hydroxide was analytical grade. Deionized water (resistivity > 10 MΩ/cm) was used. All other solvents were of the highest purity available and did not contain fluorescence impurities. Sample concentrations were adjusted to optical densities of 0.05−0.1 at the excitation wavelength. All experiments were performed at room temperature (ca. 22 °C).

B. Steady-State Fluorescence. Fluorescence spectra of nondeoxygenated, 5CN2OH and 5CN2OMe solutions, were recorded on a SLM-AMINCO-Bowman 2 luminescence spectrometer and corrected according to manufacturer specifications.[15] Excitation spectra were independent of the emission wavelength and roughly the same as the absorption spectra in the $S_0 \rightarrow S_1$ spectral region. They were collected at an emission wavelength 10 nm to the red of the excitation red edge, with 0.2 nm resolution. Likewise, emission spectra were independent of the excitation wavelength. They were collected following excitation at 290 nm, corresponding to the $S_0 \rightarrow S_2$ transition, chosen (to avoid scattering) outside the spectral window in which the emission was monitored.

Fluorescence quantum yields in a given solvent, **S**, were determined using dilute solutions of anthracene in aerated ethanol (EtOH) as a standard reference. Absolute quantum yields were subsequently calculated from the expression[35]

$$\varphi = \frac{F}{F_{ref}} \frac{A_{ref}}{A} \left[\frac{n_D(\mathbf{S})}{n_D(\mathrm{EtOH})} \right]^2 \varphi_{ref} \qquad (2.1)$$

where $\varphi_{ref} = 0.28$ is the fluorescence quantum yield of anthracene in ethanol,[36] $n_D(\mathrm{EtOH}) = 1.3594$ and $n_D(\mathbf{S})$ are the refractivity indices of EtOH and **S**, respectively,[37,38] F and F_{ref} are the areas under the fluorescence spectra of 5CN2OH (in the specified solvent) and anthracene (in ethanol), and A and A_{ref} are the corresponding absorbances of the two molecules, recorded on a Perkin-Elmer 551S UV−vis spectrophotometer at the excitation wavelength (342 nm).

C. Time-Resolved Fluorescence. To monitor PTTS in the time domain, the sample was excited by a picosecond laser at about 295 nm (the doubled frequency of the Rhodamine 6G dye laser, driven by a Nd:YAG laser), which corresponds to the $S_0 \rightarrow S_2$ electronic transition. Following photoexcitation, ultrafast relaxation to the vibrationally equilibrated S_1 state must occur, since PTTS rates do not depend on the excitation wavelength. Using a time-correlated single-photon-counting system, transient fluorescence was collected at 370 nm (R*OH), followed immediately by a measurement at 570 nm (R^*O^-). This ensures that the time axes of the acid and anion fluorescence coincide. These wavelengths were chosen in order to minimize the overlap between fluorescence signals of protonated and dissociated forms of 2OH. The instrument response function (IRF) had a full-width at half-maximum (fwhm) of about 40 ps. The full scale varied between 5 ns (measurements in water) and 100 ns, corresponding to 4.88 and 97.7 ps/channel, respectively. Time zero (for both R*OH and R^*O^-) was set to one channel before the R*OH emission peak.

III. Empirical Correlations for Steady-State Spectral Shifts

The first part of this work reports and analyzes solvent effects on the steady-state excitation and emission frequencies of 5CN2OH and 5CN2OMe. Our goal here is to differentiate between polarity and hydrogen-bonding effects, particularly to the hydroxyl group

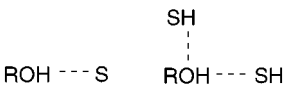

TABLE 1: Peak Excitation and Emission Frequencies of (the Acid Band of) 5-Cyano-2-naphthol and Its Methoxy Derivative in Different Solvents, with Their Corresponding Kamlet−Taft Parameters

		Kamlet−Taft parameters			excitation[d]		emission[e]	
	solvent[a]	π^{*} [b]	β[c]	α[c]	5CN2OH	5CN2OMe	5CN2OH	5CN2OMe
1	hexane	−0.11	0	0	29.41	29.33	28.28	28.22
2	c-hexane	0	0	0	29.39	29.22	28.18	28.17
3	Et_2O	0.24	0.47	0	28.92	29.31	27.2	27.72
4	EtOAc	0.45	0.45	0	28.94	29.33	26.81	27.5
5	EtOH	0.54	0.77	0.83	28.99	29.29	25.89	27.3
6	MeOH	0.60	0.62	0.93	29.04	29.29	25.93	27.12
7	ACN	0.66	0.31	0.19	29.09	29.33	26.76	27.14
8	CH_2Cl_2	0.73	0	0.3	29.26	29.19	27.33	27.46
9	$C_2H_4Cl_2$	0.73	0	0			26.98	27.43
10	TFE	0.73	0	1.51	29.57	29.53	26.0	26.82
11	DMFA	0.88	0.69	0	28.72	29.15	25.38	26.86
12	DMSO	1	0.76	0	28.69	29.15	25.11	26.55
13	water [f]	1.09	0.4[g]	1.17	29.34	29.50	25.65	26.45

[a] Acronyms: diethyl ether (Et_2O), ethyl acetate (EtOAc), ethanol (EtOH), methanol (MeOH), acetonitrile (ACN), trifluoroethanol (TFE), dimethylformamide (DMFA), dimethyl sulfoxide (DMSO). [b] From ref 17. [c] From ref 16. [d] Frequency of the red edge excitation peak (0.2 nm resolution), in 1000 cm^{-1}. [e] Peak frequency of the emission spectrum, in 1000 cm^{-1}, as obtained from a fit to the log-normal distribution.[44] From ref 15. [f] Estimated from water/MeOH or water/ACN mixtures. [g] From ref 73.

A nonprotic solvent, **S**, can act as a HB acceptor whereas a protic solvent, **S**H, may act also as a HB donor

Our analysis of the steady-state spectra is based on the empirical Kamlet−Taft parameters,[16,17] π^{*}, α, and β, which are collected in Table 1. The parameter π^{*} is a measure of solvent polarity/polarizability, whereas the "acidity" and "basicity" parameters, α and β, measure the solvent HB donating and accepting properties. Generally, the spectral shift (in the peak frequency, ν_p) is correlated by

$$\nu_p(\text{5CN2OH}) = \nu_0 + p_i\,\pi^{*} + b_i\,\beta + a_i\,\alpha \qquad (3.1)$$

where $i = 0$, 1 refers to the excitation (S_0) and emission (S_1) spectra, respectively. The coefficients p_i, b_i, and a_i reflect *solute* properties: p_i is related to its dipole moment; b_i measures its propensity to *donate* a HB, and a_i describes its tendency to *accept* a HB from the solvent in the given electronic state.

To isolate the effect of the OH group, we compare the 5CN2OH spectral shifts with those of the methoxy derivative

$$\nu_p(\text{5CN2OMe}) = \nu_0 + p_i\,\pi^{*} + a_i\,\alpha \qquad (3.2)$$

Here b_i vanishes since there is no hydrogen that could form a HB. In nonprotic solvents also $\alpha = 0$, and the shifts reflect only dipolarity effects. If the dipole moments of the two compounds are similar, we expect similar p_i values. Then, by subtraction of eqs 3.1 and 3.2 we get

$$\Delta\nu_p \equiv \nu_p(\text{5CN2OMe}) - \nu_p(\text{5CN2OH}) = \Delta\nu_0 - b_i\,\beta \qquad (3.3)$$

We have assumed that either the two compounds have similar a_i values or else the correlation is limited to solvents with $\alpha = 0$. Consequently, the solvatochromism of 5CN2OH and 5CN2OMe provides two independent routes for determining the b_i coefficient: By a multilinear regression to eq 3.1 or a linear fit to eq 3.3.

IV. Theory of Time-Resolved PTTS

The present section summarizes some of the new results pertaining to the kinetics of an excited geminate pair with different lifetimes undergoing reversible dissociation with geminate quenching.[26−29]

A. Basic Formulation. Denote by $p(*,t)$ the probability of finding the pair at time t in its bound excited state, whereas $p(r,t)$ is the probability density for the unbound excited pair to have a separation $r \geq a$. These quantities obey the spherically symmetric DSE in three dimensions,

$$\frac{\partial}{\partial t}p(r,t) = \mathcal{L}\,p(r,t) - [W_a(r) + W_q(r) + k_0']\,p(r,t) + W_d(r)\,p(*,t) \quad (4.1a)$$

$$\frac{\partial}{\partial t}p(*,t) = 4\pi\int W_a(r)\,p(r,t)\,r^2\,dr - (k_d + k_0)\,p(*,t) \quad (4.1b)$$

with the appropriate "sink terms" for association, $W_a(r)$, dissociation, $W_d(r)$, and geminate quenching, $W_q(r)$. For PTTS, it suffices to restrict all three sink terms to contact reactivity,

$$W_d(r) = \frac{k_d\delta(r-a)}{4\pi a^2} \quad W_a(r) = \frac{k_a\delta(r-a)}{4\pi a^2} \quad W_q(r) = \frac{k_q\delta(r-a)}{4\pi a^2} \quad (4.2)$$

at the reaction radius, $r = a$. The dissociation, association, and quenching rate constants are denoted by k_d, k_a, and k_q, respectively. The excited-state decay parameters of the acid and base, k_0 and k_0', are *independent* of the separation distance, r. $\mathcal{L}$ is the (three-dimensional) spherically symmetric Smoluchowski operator,

$$\mathcal{L} \equiv r^{-2}\frac{\partial}{\partial r}D(r)\,r^2 e^{-V(r)}\frac{\partial}{\partial r}e^{V(r)} \qquad (4.3)$$

with a reflective boundary condition at $r = a$.

The potential of interaction, $V(r)$, between the proton and the excited base (in units of the thermal energy k_BT) is assumed to be the Coulomb potential,

$$V(r) = -R_D/r \qquad (4.4)$$

$$R_D = e^2|z_{RO^-} z_{H^+}|/(\epsilon k_B T) \qquad (4.5)$$

Here R_D is the Debye radius, z are ionic charges, e is the electronic charge, and ϵ is the static dielectric constant of the solvent. $D = D_{RO^-} + D_{H^+}$ is the relative diffusion constant of the proton and base, which we assume to be independent of the interparticle separation r.

Initially, the excited acid is prepared by photoexcitation, hence

$$p(r,0|*) = 0 \quad p(*,0|*) = 1 \tag{4.6}$$

This initial state is denoted by $(\cdots|*)$. We are interested in the time dependence of the excited acid population, $p(*,t|*)$, as well as that of the excited anion

$$S(t|*) = 4\pi \int_a^\infty p(r,t|*)\, r^2\, \mathrm{d}r \tag{4.7}$$

These quantities correspond to the transient experimental signals. When $V(r) \neq 0$, eq 4.1 cannot be solved analytically, but it is possible to obtain its exact long-time asymptotic behavior.[27,28]

B. Definitions of Derived Quantities. The resulting expressions depend on several steady-state rate and equilibria coefficients:

(I) the diffusion-controlled rate coefficients for separation and approach

$$k_{-\mathrm{D}} \equiv k_{\mathrm{D}}\, \mathrm{e}^{V(a)} \quad k_{\mathrm{D}} \equiv 4\pi\, D a_{\mathrm{eff}} \tag{4.8}$$

(II) two steady-state "off" rate coefficients

$$k_{\mathrm{off}} = \frac{k_{\mathrm{d}} k_{-\mathrm{D}}}{k_{\mathrm{a}} + k_{-\mathrm{D}} + k_{\mathrm{q}}} \quad k_{\mathrm{off}}^{\mathrm{q}} = \frac{k_{\mathrm{d}}(k_{-\mathrm{D}} + k_{\mathrm{q}})}{k_{\mathrm{a}} + k_{-\mathrm{D}} + k_{\mathrm{q}}} \tag{4.9}$$

(III) two association equilibrium coefficients

$$K_{\mathrm{eq}} \equiv k_{\mathrm{a}} \mathrm{e}^{-V(a)}/k_{\mathrm{d}} \quad K_{\mathrm{eq}}^{\mathrm{q}} \equiv (k_{\mathrm{a}} + k_{\mathrm{q}}) \mathrm{e}^{-V(a)}/k_{\mathrm{d}} \tag{4.10}$$

In the above expressions, the effective contact radius is defined by

$$a_{\mathrm{eff}} \equiv \left(\int_a^\infty \mathrm{e}^{V(r)} r^{-2}\, \mathrm{d}r\right)^{-1} = \frac{R_{\mathrm{D}}}{1 - \exp(-R_{\mathrm{D}}/a)} \tag{4.11}$$

In addition, two different modified effective radii are introduced

$$a'_{\mathrm{eff}} \equiv \frac{k_{\mathrm{a}} a_{\mathrm{eff}}}{k_{\mathrm{a}} + k_{-\mathrm{D}} + k_{\mathrm{q}}} \quad a_{\mathrm{eff}}^{\mathrm{q}} \equiv \frac{(k_{\mathrm{a}} + k_{\mathrm{q}}) a_{\mathrm{eff}}}{k_{\mathrm{a}} + k_{-\mathrm{D}} + k_{\mathrm{q}}} \tag{4.12}$$

and their definitions parallel those of k_{off} and $k_{\mathrm{off}}^{\mathrm{q}}$.

C. Asymptotic Behavior. In the case of two different lifetimes the asymptotic behavior undergoes a transition, which depends on the sign of the dimensionless parameter

$$B \equiv \frac{(k'_0 - k_0 - k_{\mathrm{off}}^{\mathrm{q}}) 4D}{(k_{\mathrm{off}}\, a'_{\mathrm{eff}})^2} \tag{4.13}$$

Under our experimental conditions $B < 0$, so that

$$k_0 + k_{\mathrm{off}}^{\mathrm{q}} > k'_0 \tag{4.14}$$

Since the diffusing separated pair is relatively long-lived, diffusion-controlled re-encounters lead to power law asymptotics

$$p(*,t|*) \sim Z^2 \frac{K_{\mathrm{eq}}}{(4\pi D t)^{3/2}} \mathrm{e}^{-k'_0 t} \tag{4.15a}$$

$$S(t|*) \sim Z\left\{1 + \frac{[K_{\mathrm{eq}}^{\mathrm{q}}(k_0 - k'_0) + k_{\mathrm{q}}\, \mathrm{e}^{-V(a)}]}{4\pi D} \frac{Z}{\sqrt{\pi D t}}\right\} \mathrm{e}^{-k'_0 t} \tag{4.15b}$$

where Z is the ultimate escape probability

$$Z \equiv \frac{k_{\mathrm{off}}}{k_{\mathrm{off}}^{\mathrm{q}} + k_0 - k'_0} \tag{4.16}$$

Several remarks are appropriate to the above asymptotic behavior:

(a) Both acid and base decay with the lifetime of the *anion*, $\tau'_0 \equiv 1/k'_0$.

(b) For equal lifetimes and no quenching, the "effective" signal of the base, $S(t|*)\exp(k'_0 t)$, increases monotonically to the ultimate escape probability, Z. In the more general case discussed here, it goes through a maximum and approaches Z from above with a $1/\sqrt{t}$ asymptotic law.[21] Note how *both* $k_0 - k'_0$ and k_{q} contribute to this maximum.

(c) As compared with the simpler case of equal lifetimes and no quenching, the acid signal is simply multiplied by Z^2.

(d) Finally, if $B > 0$ the diffusing state decays faster than the bound state. The effect of diffusion then diminishes to the extent that the asymptotic behavior becomes purely exponential.[27,28]

D. Steady-State Attributes. Using the parameters of the time-resolved kinetics, one may evaluate three quantities usually obtained from steady-state measurements:

(I) The excited-state acid equilibrium constant, K_{a}^*, is calculated from the rate parameters according to

$$K_{\mathrm{a}}^* = 10^{27} k_{\mathrm{d}} \exp(-R_{\mathrm{D}}/a)/(N_{\mathrm{A}} k_{\mathrm{a}}) \tag{4.17}$$

where N_{A} is Avogadro's number. It is K_{eq}^{-1} for the excited-state reaction represented in the conventional units of molar. As usual, $\mathrm{p}K_{\mathrm{a}}^* = -\log K_{\mathrm{a}}^*$.

(II) The steady-state recombination rate coefficient, k_{on}, is given by

$$k_{\mathrm{on}} = \frac{k_{\mathrm{D}} k_{\mathrm{a}}}{k_{\mathrm{a}} + k_{-\mathrm{D}} + k_{\mathrm{q}}} \tag{4.18}$$

This expression is analogous to the definition of k_{off} in eq 4.9. Moreover, it is easy to check that $k_{\mathrm{on}}/k_{\mathrm{off}} = K_{\mathrm{eq}}$. Thus the *same* equilibrium constant is obtained from the ratio of the steady-state and the microscopic (contact) rate parameters.

(III) The absolute fluorescence quantum yields (AQY) of the acid and base forms, φ and φ', are defined by

$$\varphi \equiv k_{\mathrm{f}} \int_0^\infty p(*,t)\, \mathrm{d}t \tag{4.19a}$$

$$\varphi' \equiv k'_{\mathrm{f}} \int_0^\infty S(t)\, \mathrm{d}t \tag{4.19b}$$

where the corresponding radiative (fluorescence) rate constants are k_{f} and k'_{f}. For the initially bound state, one obtains[27,28]

$$\frac{k_{\mathrm{f}}}{\varphi(*)} = k_{\mathrm{off}}^{\mathrm{q}} + k_0 + k_{\mathrm{off}} \sqrt{a'^{\,2}_{\mathrm{eff}} k'_0 / D} \tag{4.20a}$$

$$\frac{k'_{\mathrm{f}}}{\varphi'(*)} = \frac{k'_0}{k_{\mathrm{off}}}\left[k_{\mathrm{off}}^{\mathrm{q}} + k_0 - \left(k_0 + \frac{k_{\mathrm{d}} k_{\mathrm{q}}}{k_{\mathrm{a}} + k_{\mathrm{q}}}\right)\sqrt{a_{\mathrm{eff}}^{\mathrm{q}\,2} k'_0 / D}\right] \tag{4.20b}$$

With AQY obtained from steady-state spectra and rate parameters derived from transient data, one may determine the

TABLE 2: Parameters Used in Fitting the Time-Resolved Fluorescence Decay of 5CN2OH to Eq 4.1 in Various Solvents[a]

solvent	R_D, Å	D_{H^+}, 10^{-5} cm^2/s	D_{RO^-}, 10^{-5} cm^2/s	τ_0', ns^{-1}	k_d, ns^{-1}	κ_r, Å/ns	κ_q, Å/ns
EtOH	23.1	1.29	0.65	11.4	0.135	9.0	2.5
MeOH	17.2	2.37	1.29	10.1	0.23	16	2.3
DMFA	15.4	1.26	0.83	17.7	0.115	16	0
DMSO	12.1	0.65	0.35	22.6	0.25	1.2	0
water	7.28	9.41	0.75	7.4	45	26?	25

[a] In all solvents we have taken $a = 5.5$ Å and $\tau_0 = 5.7$ ns. Only k_d, $k_r = 4\pi a^2\kappa_r$, and $k_q = 4\pi a^2\kappa_q$ were used as adjustable parameters.

radiative rate constants. These then enable one to obtain the nonradiative decay rates, k_{nr}, using

$$k_0 = k_f + k_{nr} \tag{4.21a}$$

$$k_0' = k_f' + k_{nr}' \tag{4.21b}$$

V. Fitting Procedures

A. Parameter Determination. The experimental data were fitted to the numerical solution of the time-dependent DSE, eq 4.1, using a Windows95 application for solving the spherically symmetric diffusion problem (SSDP ver. 2.55).[39] While building a decay curve requires the values of *eight* independent parameters, only *three* are adjusted to fit the data. These are the rate coefficients k_a, k_d, and k_q. While the number of adjustable parameters does not exceed that of the simplest corresponding kinetic scheme, we are able to fit the highly nonexponential decay curves emanating from the diffusive nature of the reaction. Moreover, the different rate parameters influence different time windows of the observed kinetics. For example, k_d affects only the initial slope of the ROH decay curve, k_a determines its long-time tail, and k_q determines the shape of the R*O$^-$ signal near its peak.

Of the various parameters collected in Table 2, five were estimated from independent experimental data as follows. The contact radius, $a = 5.5$ Å, is a typical literature value.[23] The Debye radius, R_D, was calculated from eq 4.5, with z_{H^+}, $= 1$, $z_{RO^-} = -1$. For 5CN2OH at room temperature $R_D = 566/\epsilon$ Å. The proton diffusion constant, D_{H^+}, has been estimated from conductivity data[40] and extrapolated to infinite dilution. The anion diffusion constant, D_{RO^-}, was assumed to be about 0.75×10^{-5} cm^2/s in water (and independent of the electronic state). This value is within the range $(0.55-0.95) \times 10^{-5}$ cm^2/s, observed for various aromatic compounds.[41] It was scaled to its value in solvent **S** using the viscosity ratio η_{H_2O}/η_S. The relative diffusion coefficient, $D = D_{H^+} + D_{RO^-}$, was subsequently used in the program.

The excited-state lifetime of the anion, $\tau_0' \equiv 1/k_0'$, was determined directly from the long-time exponential decay of the R*O$^-$ fluorescence signal (see below). Determination of the R*OH lifetime, $\tau_0 \equiv 1/k_0$, is more problematic, because of PTTS. Measurements under acidic conditions lead to quenching by protons. For solvents in which 5CN2OH does not dissociate (e.g., acetonitrile), we typically find that the difference in R*OH lifetimes between 5CN2OH and 5CN2OMe does not exceed 10%. We have therefore used the major fluorescence decay component of 5CN2OMe, 5.7 ns, as an estimate for τ_0 in *all* solvents. This value is close to the lifetime of 2OH in acetonitrile.[42]

Computations were carried out for the above parameters, on a spatial grid extending from $a = 5.5$ to 1500 Å (which, for the present parameters, is essentially infinity) using 500 grid points and a logarithmic time scale (from 5 ps to 100 ns). The three contact rate parameters were adjusted manually. In our previous notations,[23] these parameters are $\kappa_d = k_d$, $\kappa_r = k_a/(4\pi a^2)$ and $\kappa_q = k_q/(4\pi a^2)$. We usually started with $k_a = 0$ and $k_q = 0$, adjusting k_d to the initial decay. Then k_a was gradually increased until the nonexponential tail was adequately fitted. Nonadequate fitting of the R*OH curve by the above procedure, with a concomitant nonexponential decay of R*O$^-$, signals the involvement of quenching. Subsequently, k_q is increased until ultimate agreement is obtained. To summarize, only three *adjustable* kinetic parameters, k_d, k_a, and k_q, are required to analyze the fluorescence decay curves of *both* acid and anion.

B. Data Manipulation and Corrections. A quantitative work requires several procedures of data correction and manipulation which are described below.

I. Smoothing. To facilitate visualization of the long-time behavior, the experimental data were smoothed iteratively by averaging adjacent data points. Thus if (t_i, I_i) are ordered time and fluorescence intensity data points, they are replaced iteratively by $((t_i + t_{i+1})/2,(I_i + I_{i+1})/2)$, but only past the maximum in I_i. This smoothing algorithm eliminates the high-frequency noise but does not otherwise influence the center of gravity of the data.

II. Scattered Light. Although precautions were taken to avoid background and scattered stray light, we have found it necessary to subtract $I_{scat} = 1-3$ counts from the measured anion signal to compensate for background photons. The replacement of $I(t)$ by $I(t) - I_{scat}$ is particularly important for anion fluorescence, which is monitored to longer times.

III. Fluorescence Impurities. In water solutions, a long-lived nonexponential component contributing several percent to the R*OH signal was observed. The average lifetime (ca. 3 ns) of this component was smaller than that of R*O$^-$. Thus it could not be ascribed to the appearance of the R*O$^-$ signal at 370 $\pm$ 5 nm. As in previous work,[14] we attribute this component to either (a) 5CN2OH oligomers whose solubility decreases significantly from methanol to water and/or (b) impurities that do not undergo excited-state PTTS, such as 5CN2OMe—the precursor of 5CN2OH in the multistep synthesis.[13]

IV. Band Overlap. Normalized spectra of 5CN2OH in methanol, methanol with sulfuric acid (pure R*OH), and methanol with sodium hydroxide (pure R*O$^-$) are presented in Figure 1. The dash−dotted vertical lines mark the wavelengths at which time-resolved measurements were performed, 370 nm (R*OH) and 570 nm (R*O$^-$). Although these were chosen to minimize the overlap between the two bands, there is evidently a long red tail of the R*OH signal under the R*O$^-$ band. In the spectral bandwidth 565−575 nm its integrated intensity is about 4.5% of the overall signal. Without taking this into account, the experimental rise time of R*O$^-$ in methanol and ethanol is faster than the corresponding decay of R*OH; see Figure 2. If $\alpha_{over} \approx 0.045$ denotes this fractional overlap and $S(t|*)$ and $p(*,t|*)$ are the theoretical probabilities for observing the excited anion and acid, then we compare the anion fluorescence signal with $(1 - \alpha_{over})S(t|*) + \alpha_{over}p(*,t|*)$. In the nonalcoholic solutions (DMSO, DMFA, and water), no such correction was necessary. Unlike the case of hydroxypyrenetrisulfonate,[23] no appreciable R*O$^-$ signal was observed at the wavelength of R*OH measurements in the nonaqueous solutions.

V. Convolution. The theoretical decay curves were convoluted with the experimental instrument response function (IRF) measured using the same time-scale as the corresponding R*OH and R*O$^-$ kinetics. As in previous work,[23,43] we found it necessary to increase manually the IRF width by about 10%.

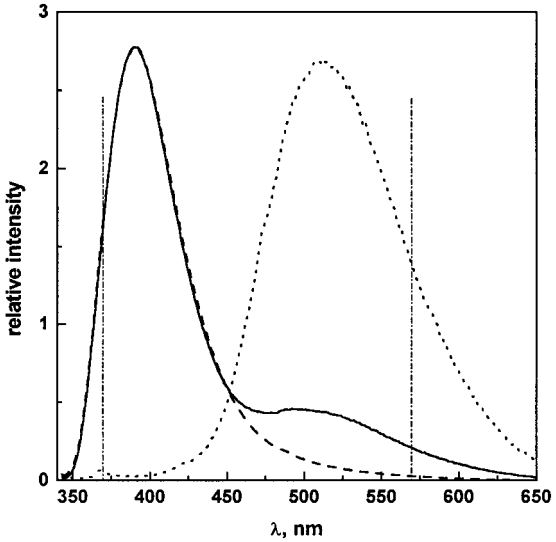

Figure 1. Normalized emission spectra of 5CN2OH in methanol (solid line), methanol with sulfuric acid (dashed line), and methanol with sodium hydroxide (dotted line). Vertical dashed−dotted lines refer to characteristic R*OH (370 nm) and R*O$^-$ (570 nm) wavelengths at which time-resolved measurements were performed.

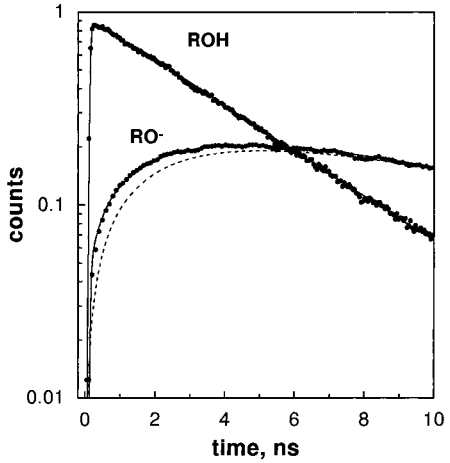

Figure 2. Experimental (dots) and theoretical (lines) fluorescence decay curves of 5CN2OH in methanol. The dashed line refers to R*O$^-$ decay curve calculated without taking into account the overlap between the R*OH and R*O$^-$ bands (see text for detail).

This is due to our optical setup, which involves small-angle front-surface fluorescence from cells of 5 mm optical path.

VI. Results

We begin by analyzing the solvatochromic shifts in the steady-state excitation and emission spectra using the empirical Kamlet−Taft approach. For solvents in which anion fluorescence due to PTTS is observed, we analyze the time-resolved fluorescence data using the DSE for depicting excited-state reversible geminate recombination with different lifetimes and quenching.

A. Steady-State Spectra. Fluorescence excitation spectra for 5CN2OH and 5CN2OMe in different solvents are shown in Figure 3 as bold and dashed lines, respectively. These are similar to the absorption spectra (not shown). The red edge peak frequencies, corresponding to the $S_0 \rightarrow S_1$ transition, are collected in Table 1. Except for water, no evidence for ground-state protolytic dissociation of the 5CN2OH acid is observed, commensurate with its high pK_a value (estimated 8.75 in water[13]). While the solvents in the table are ordered by

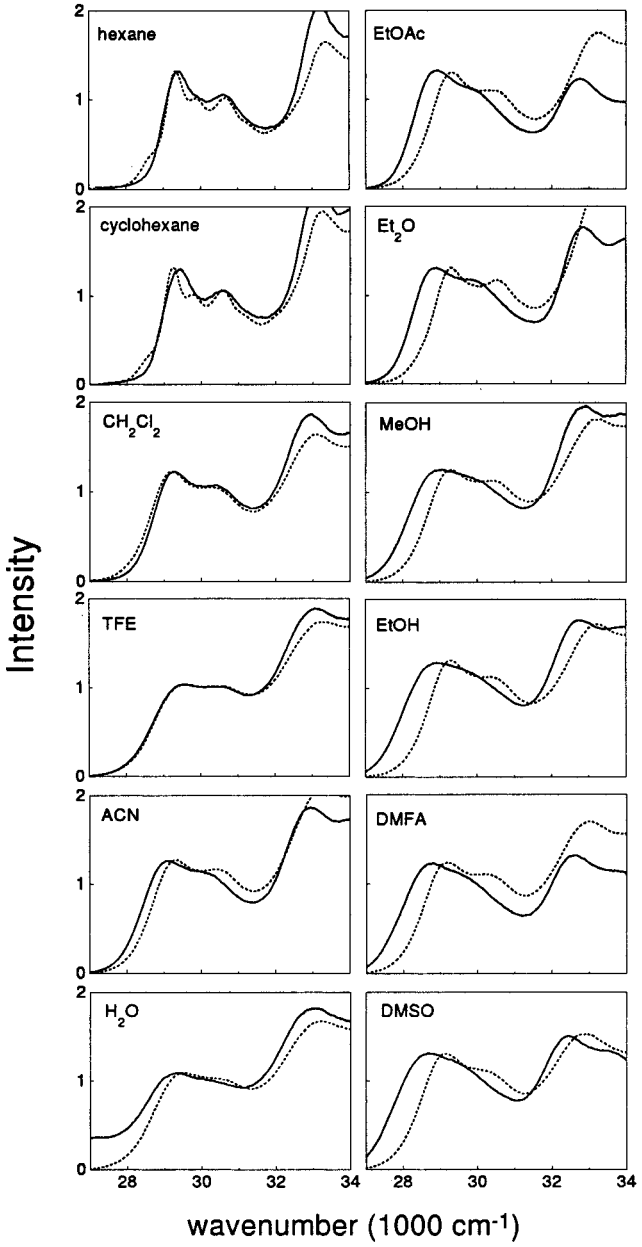

Figure 3. Fluorescence excitation spectra of 5-cyano-2-naphthol (full lines) and its methoxy derivative (dashed lines) in the different indicated solvents. Frequencies of the red-edge peaks are collected in Table 1.

increasing π^*, the data in the columns of the figure correspond to increasing red shifts between 5CN2OH and its methoxy derivative. This correlates with β, not with π^*.

Fluorescence emission spectra of 5CN2OH in several solvents are shown in Figure 4. The acid band appears in the region 365−415 nm and the anionic base band around 500−550 nm. This gives a clear indication that excited-state PTTS to water *and* a variety of organic solvents does take place during the excited-state lifetime of the chromophore. Of course, there are many more solvents in which no PTTS occurs, and these possess a single ROH band which, nevertheless, exhibits solvatochromic shifts.

Figure 5 shows the ROH emission band in 10 of the solvents investigated, regardless of whether PTTS takes place. As for excitation (Figure 3), 5CN2OH spectra (full lines) are compared with those of 5CN2OMe (dashed lines). Again, solvents in the columns of the figure are ordered by the increasing red shift between the two compounds, which is seen to follow the order

TABLE 3: Absolute Quantum Yields, φ, and Anion Emission Frequencies, $\nu_p(RO^-)$, of 5CN2OH in Different Solvents

				φ		τ_f, ns		k_{nr}, ns^{-1}	
solvent	ϵ^a	$\Delta G_t(H^+)$,[b] kJ/mol	$\nu_p(RO^-)$, 1000 cm^{-1}	ROH	RO$^-$	ROH	RO$^-$	ROH	RO$^-$
EtOH	24.3	11		0.20	0.019	22	98	0.13	0.077
MeOH	32.7	10	19.46	0.18	0.055	19.5	62	0.12	0.083
DMFA	36.7	−18	18.38	0.27	0.12	17	28	0.12	0.021
MFA	182.4	−20	18.87						
DMSO	46.7	−19	18.31	0.17	0.40	16	35	0.11	0.016
water	78.4	0	19.29	0.0015	0.070	18	84	0.12	0.123

[a] Static dielectric constant, from ref 38. [b] Proton free energy of transfer, from ref 38.

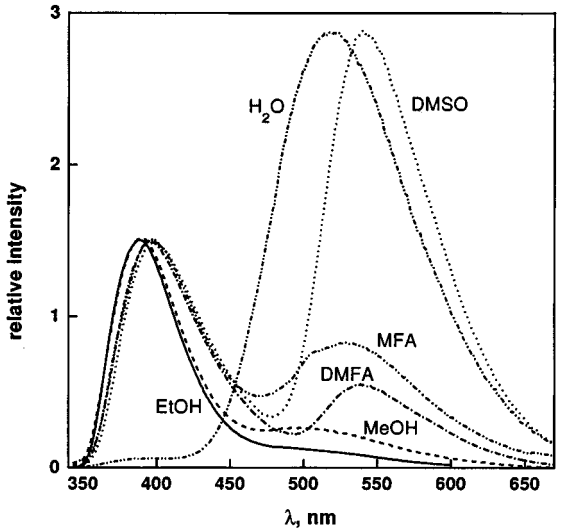

Figure 4. Dual-fluorescence of 5-cyano-2-naphthol in solvents to which excited-state proton transfer takes place. The low-energy anion band has been fitted to a log-normal line shape (not shown), and the peak frequencies are collected in Table 3.

of β (and not π^*). Unlike the excitation spectra, it is possible here to adopt a more quantitative approach for extracting the peak frequencies. The line shapes are fitted by the log-normal distribution,[44] as seen by the dotted lines. For the least polar solvents, hexane and cyclohexane, these fits average over the observed vibrational structure. In the more polar solvents no such structure is observed, and the log-normal function provides an adequate fit. From it, the peak frequency, ν_p, is extracted using previously detailed procedures,[45] and collected in Table 1. These data are essentially identical to those in our preliminary report.[15] A similar procedure is applied to extract the peak frequencies of the anionic band from the spectra of Figure 4. These data are collected in Table 3.

The solvatochromic shifts in the $S_0 \rightarrow S_1$ excitation band and in the ROH and RO$^-$ emission bands are depicted in Figures 6−8, respectively. Consider first the ROH band in Figures 6 and 7. In both figures, panel a shows that the 5CN2OMe frequency shifts (open symbols) can be explained by polarity effects, whereas the 5CN2OH shifts (plus signs) cannot. To obtain a good correlation with π^*, protic solvents had to be excluded from the excitation (squares, Figure 6) but not from the emission data set (Figure 7). In the first case the correlation line, eq 3.2, is restricted to solvents with $\alpha = 0$, whereas in the second case it is unrestricted, and we obtain $a_1 = 0$. Panel b shows a fit of the difference frequency to eq 3.3. Again, protic solvents (full squares) deviate from the correlation line for the excitation frequencies. In the emission, chloroaliphatics deviate and are hence excluded from the correlation in Figure 7. With the exclusion of these data points, one obtains a good correlation with the solvent basicity parameter, β. The coefficients, p_i, b_i, and a_i, are collected in Table 4. We estimate the error in these coefficients by 50−100 cm^{-1}.

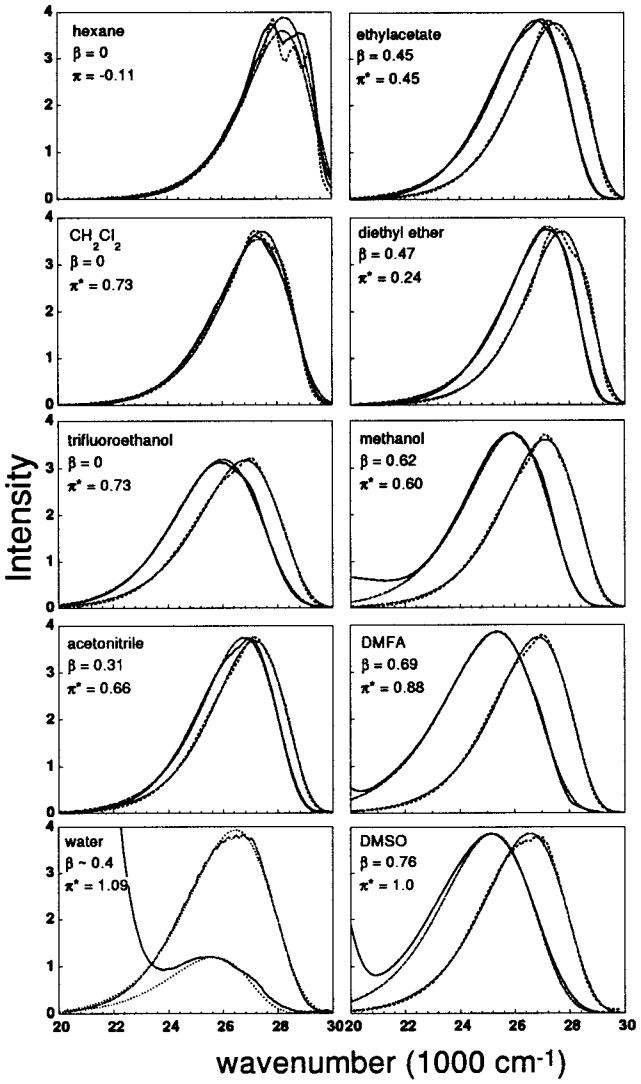

Figure 5. Fluorescence emission spectra of the acid band of 5-cyano-2-naphthol (full lines) and its methoxy derivative (dashed lines) in the different indicated solvents. Dotted curves are best-fits to a log-normal line shape. Peak frequencies extracted from these fits are collected in Table 1.

The RO$^-$ frequencies (Table 3) correlate predominantly with the solvent HB donating power, α. The regression line in Figure 8 obeys the equation $\nu_p(RO^-) = 18.37 + 0.94\alpha$ (in 1000 cm^{-1}), with a correlation coefficient of 0.96. The data point for MFA deviates considerably and is hence not included. Table 3 also collects some of the acid and anion AQY, as determined experimentally from eq 2.1.

B. Time-resolved Fluorescence. Figure 9 shows time-resolved fluorescence of 5CN2OH in four solvents to which it

TABLE 4: Kamlet−Taft Coefficients for 5-Cyano-2-naphthol, Its Methoxy Analog, and Anion

		excitation			emission		
molecule	equation	$-p_0$, cm^{-1}	$-b_0$, cm^{-1}	a_0, cm^{-1}	$-p_1$, cm^{-1}	$-b_1$, cm^{-1}	a_1, cm^{-1}
5CN2OH	3.1	150	680	270	1600	1950	0
	3.3		690			1820	
5CN2OMe	3.2	90		190	1600		0
	nonprotic	120					
5CN2O$^-$	3.2				0		940

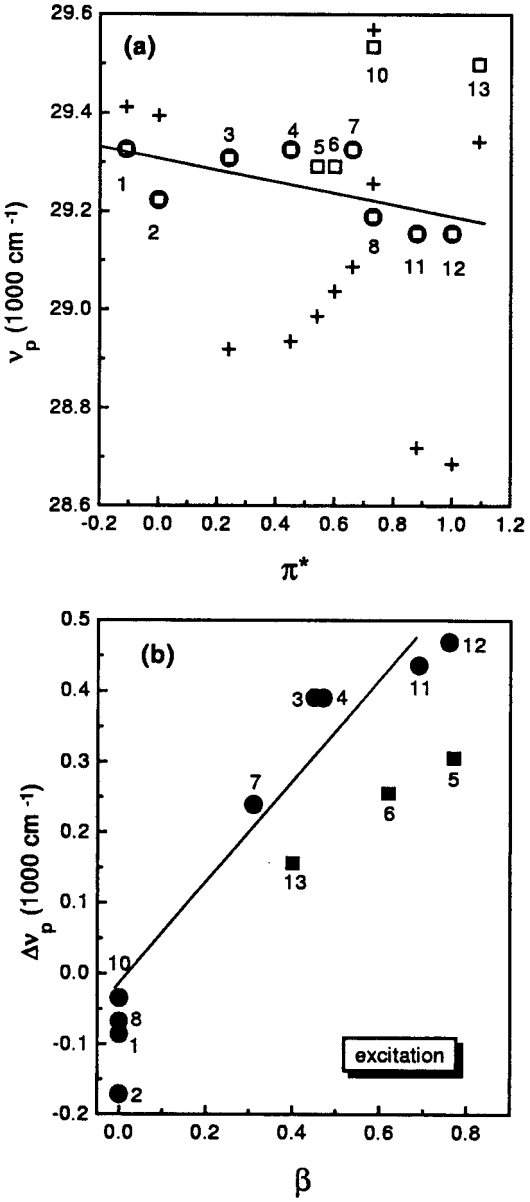

Figure 6. Solvatochromism of the red-edge excitation band: (a) 5CN2OMe (open symbols) and 5CN2OH frequencies (plus symbols); (b) 5CN2OMe − 5CN2OH frequency difference (closed symbols). Solvents are numbered according to their order in Table 1. Squares represent protic solvents, which are excluded from the correlation line; see Table 4.

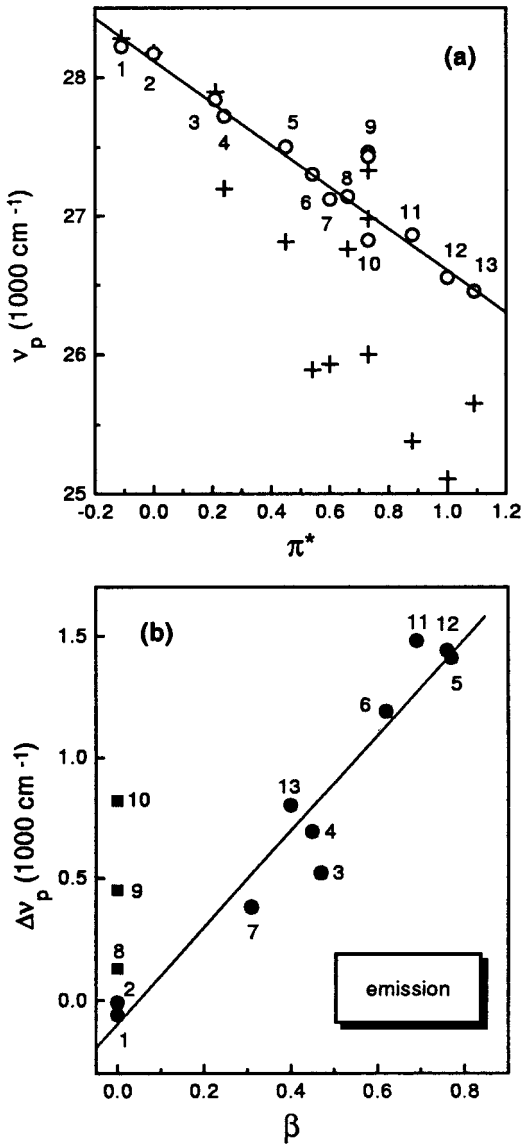

Figure 7. Solvatochromism of the peak emission: (a) 5CN2OMe (open circles) and 5CN2OH (acid band, plus symbols) frequencies; (b) 5CN2OMe − 5CN2OH frequency differences (closed symbols). Solvents are numbered according to their order in Table 1. Squares in (b) represent chloroaliphatic solvents, which are excluded from the correlation line; see Table 4.

transfers the proton during its excited-state lifetime. The data are processed as described in section V.B and multiplied by $\exp(t/\tau_0')$, where τ_0' is the lifetime of the anion. This produces "effective" probabilities for the excited-state species. We see that while the effective acid signal decays to zero, that of the anion rises and approaches the ultimate escape probability Z, eq 4.16. The lines show the fit to the numerical solution of eq 4.1 with fitting parameters collected in Table 2. Only the values of the three rate parameters, k_d, k_a, and k_q, were adjusted to obtain these fits. The other parameters were taken from independent measurements, as discussed above. Various rate and equilibrium constants derived from these elementary parameters (section IV) are collected in Table 5.

Of the four solvents, alcohols show a quenching effect whereas the data in the nonprotic solvents may be fitted with $k_q = 0$. This effect is best recognized from the shape of the "effective" anion fluorescence signal, $S(t|^*)\exp(t/\tau_0)$, near its peak. Past this peak, it decays with the $t^{-1/2}$ law, eq 4.15b. Unlike the case of 1-naphthol,[21,22,28] the effect of quenching

TABLE 5: Derived Parameters Obtained from Those of Table 2 Using Definitions in Section IV[a]

solvent	k_{-D}, 10^3 Å^3/ns	k_a, 10^3 Å^3/ns	k_q, 10^3 Å^3/ns	k_{off}, ns^{-1}	k^q_{off}, ns^{-1}	k_{on}, M^{-1} ns^{-1}	Z	pK^*_a
EtOH	0.86	3.4	0.95	0.022	0.047	22	0.165	3.0
MeOH	3.6	6.1	0.87	0.079	0.098	28	0.45	2.6
DMFA	2.6	6.1	0	0.035	0.035	18	0.23	2.7
DMSO	1.9	0.45	0	0.20	0.20	2	0.605	0.94
water	34	9.9?	9.5	29	37	14	0.78	−0.3

[a] The units of the bimolecular rate coefficients correspond to a single pair, except for k_{on}, which was converted to molar units to allow comparison with bulk measurements.

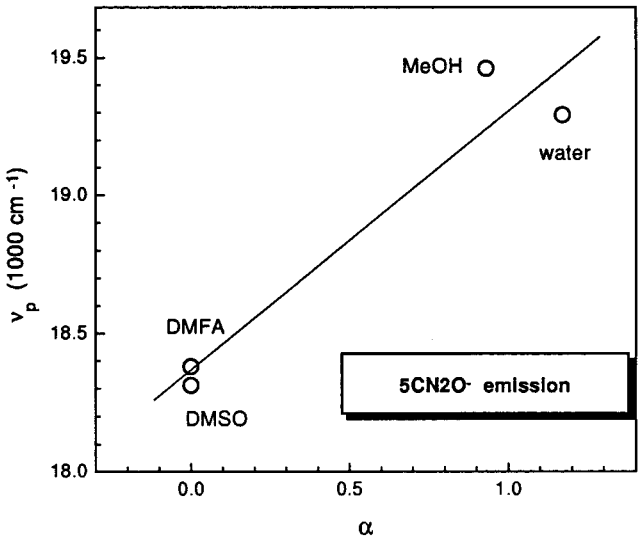

Figure 8. Solvatochromism in the 5-cyano-2-naphtholate emission peak, for an anion formed by direct acid excitation.

here is not sufficiently strong to produce a noticeable peak. This might limit the accuracy of k_q.

The power-law asymptotic decay of the acid fluorescence, eq 4.15a, can be recognized when $p(*,t|*)\exp(t/\tau_0')$ is plotted on a log−log scale, as in Figure 10. Note that, in agreement with eq 4.15a, the power-law decay becomes visible only when the acid signal is corrected using the lifetime of the *base*. This characterizes the behavior in the experimentally accessible $B < 0$ regime. With the exception of DMSO, sample purity and signal/noise ratio are insufficient for generating data all the way to the asymptotic limit (dash−dotted curve), which affects the accuracy of k_a. In comparison with previous measurements in methanol,[14] we obtain the same k_d but a considerably larger k_a. This may be attributed to the neglect of quenching in the earlier work.[14]

The data for water are shown in Figure 11. Dissociation here occurs considerably faster, within the IRF (dashed curve). With the exclusion of the long-time tail, which we attribute to aggregation, a good fit is obtained for both acid and base with the same parameter set. Nevertheless, the error bars on k_a must be larger than for the other solvents.

C. Derived Steady-State Attributes. As discussed in section IV.D, one may use the fitted rate parameters to calculate steady-state rate and equilibrium constants:

(I) The excited-state equilibria constants in the different solvents are calculated from eq 4.17 and collected in Table 5. In water, we obtain $pK^*_a = -0.3$, in comparison with a value[14] of −0.75 (or −1.2 using the Förster cycle[13]). The Förster cycle gives inaccurate results due to neglect of excited-state relaxation. Our results in water might be inaccurate due to the limited time resolution.

(II) The steady-state recombination rate constants, k_{on}, are calculated from eq 4.18 and collected in Table 5. We find values between 2 and 3×10^{10} M^{-1} s^{-1}, except for water and DMSO, where the values are smaller. Unfortunately, the value in water may be in error by as much as a factor of 2 due to the apparent aggregation problems. On the other hand, fluorometric titrations are difficult to perform in nonaqueous solutions. Subsequently, there are no available steady-state recombination rate coefficients for 5CN2OH with which to compare our results (however, see Discussion).

(III) The radiative lifetimes and nonradiative decay rate constants for both acid and base were calculated from eqs 4.20 and 4.21 and collected in Table 3. Unlike the solvent dependence of τ_f, which (at least for the acid) is relatively weak, k_{nr} exhibits strong solvent dependence, which will be discussed below.

VII. Discussion

The present work reports on steady-state and time-resolved fluorescence measurements of a novel "super" photoacid, 5-cyano-2-naphthol (5CN2OH). This compound is sufficiently acidic in its excited state to transfer its proton to various solvents within its excited-state lifetime. Hence it allows the study of solvent effects on the spectral shifts and kinetic parameters, which we shall now discuss.

A. Spectral Shifts. Excited-state PTTS begins with photoexcitation, which sets the stage for the subsequent proton-transfer step. Although we have not performed ultrafast time-resolved experiments on this system, we can infer about the primary steps from the solvatochromic shifts in the excitation and emission spectra. These are summarized by the Kamlet−Taft coefficients in Table 4, which separate empirically hydrogen-bonding effects (a_i and b_i) from dipole−dipole interactions (p_i). To check the reliability of this approach for the present data, we have compared the analysis for 5CN2OH and 5CN2OMe. The latter has no OH group donating a HB to solvent. Commensurate with this fact, we find that $b_i = 0$, whereas the other two coefficients assume values similar to those for 5CN2OH. Consequently, the difference in frequencies between the two compounds depends only on β, eq 3.3, with b_i values similar to those obtained from the three-parameter regression to the 5CN2OH shifts. Thus the comparison of solvatochromic shifts between the two compounds (a) corroborates the analysis by an independent measurement of the methoxy shifts and (b) demonstrates that the effect of β is due to a single HB namely, the ROH···**S** interaction.

Our interpretation of the solvatochromic coefficients in Table 4 is based on the following considerations. By the Franck−Condon approximation, the solvent conformation does not change during the electronic transition. For a given solvent conformation, the change in the molecular electron density upon excitation can make the property under consideration (dipole moment, HB) stronger or weaker, leading to red or blue spectral shifts. This is indicated in the *sign* of the corresponding solvatochromic coefficient (a_i, b_i, or p_i). Their relative *magnitude* in absorption vs emission indicates whether nuclear (solvent)

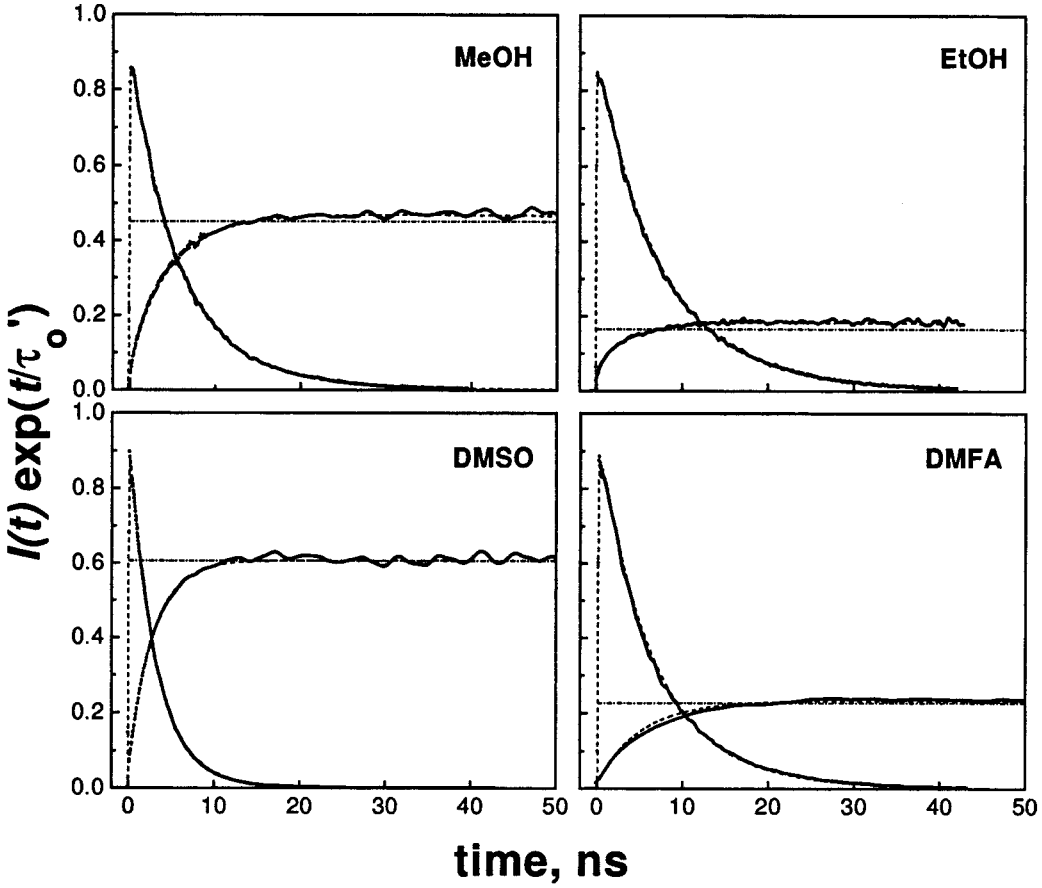

Figure 9. Time-resolved kinetics of 5CN2OH in organic solvents. Experimental data (points, normalized to the theoretical amplitudes) are compared with the numerical solution of the DSE (dashed lines), using the parameters of Table 2, after convolution with the IRF for both acid (decaying) and anion (rising) fluorescence. Note that all the lines are corrected for the lifetime of the *anion*. The dash−dotted line is the ultimate dissociation probability, *Z*, From eq 4.16.

rearrangement following photoexcitation reinforces or weakens the corresponding interaction.

Consider first "nonspecific" solvation due to dipole−dipole interactions. The observed red shifts (negative p_i) suggest that the dipole moment increases upon excitation, so that stabilization by dipole−dipole interactions is larger in S_1 than in S_0. The continuum theory for "nonspecific" dipolar effects is well documented,[46] and used extensively to extract dipole moments from observed shifts in absorption and emission spectra.[47] Generally speaking, dipole moments are vectors assuming the values $\vec{\mu}_0$ and $\vec{\mu}_1$ in the S_0 and S_1 states, respectively. The shifts in the absorption and emission spectra are approximately proportional to the scalar products $\vec{\mu}_0 \cdot (\vec{\mu}_1 - \vec{\mu}_0)$ and $\vec{\mu}_1 \cdot (\vec{\mu}_1 - \vec{\mu}_0)$, respectively.[47] Thus, when $\vec{\mu}_1$ and $\vec{\mu}_0$ are parallel, the expressions simplify. This might not be a bad assumption for 5CN2OH, where the direction of the dipole moment is determined by the OH and CN groups and is thus expected to vary only slightly upon excitation. Under these conditions, the ratio of the shifts is equal to the ratio of (the magnitudes of the) dipole moments, μ_i. Assuming that the relevant shifts are only those contributed from the π^* dependence, we conclude that approximately

$$p_1/p_0 = \mu_1/\mu_0 \qquad (7.1)$$

The experimental p_i values suggest that μ_0 (for either 5CN2OH or 5CN2OMe) is very small, whereas μ_1 is larger by about an order of magnitude.

In comparison, the large $-b_i$ value shows that solvation is dominated by *specific interactions*: The single ROH···**S** interaction ($b_i\Delta\beta$) accounts for nearly half of the solvent-induced Stokes shift in S_1 and more than that in S_0. The bathochromic (red) shift, $b_i < 0$, indicates that this HB is stronger in S_1 than in S_0.

In contrast to the effect of β, increasing α results in a hypsochromic (blue) shift, hence $a_0 \geq 0$. This is attributed to a RHO···H**S** bond that forms in protic solvents. The blue shift indicates that this bond is weaker in the excited state. Both shifts originate from electron density migration to the aromatic ring upon excitation. The enhanced positive charge on the OH group makes it a better HB donor and a worse HB acceptor. Our interpretation of α is corroborated by the observation that the a_i values for 2OH are similar to those of 5CN2OH.[48] Thus, either the cyano group is not a good HB acceptor or else its strength is independent of the excitation state.

Consider next the effect of excitation on the HB geometry. We find that $-b_1 > -b_0$ whereas $a_1 = 0$, suggesting that solvent relaxation after excitation leads to significant strengthening of the R*OH···**S** bond and essentially to the cleavage of the R*HO···H**S** bond.

The above conclusions are in agreement with two observations discussed in the literature. (a) From the analysis of the rotational−vibrational spectrum of naphthol−ammonia gas-phase dimers[49,50] it was concluded that upon excitation to S_1, the R*OH···NH_3 bond shortens by as much as 0.2 Å. (b) Recent time-resolved IR measurements of the CO frequency of coumarin 102 in $CHCl_3$ show a strong blue shift on a 200 fs time scale.[51] This indicates that the CO···$HCCl_3$ bond breaks upon excitation.

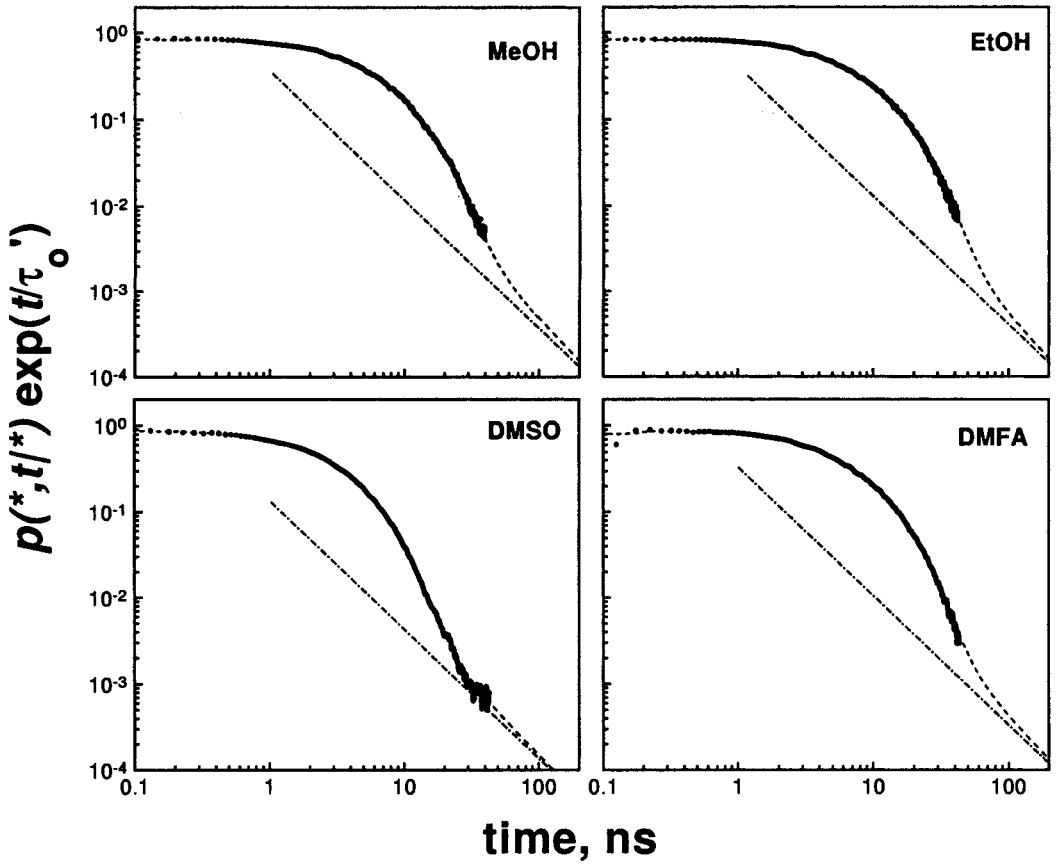

Figure 10. Time-resolved kinetics of 5CN2OH in organic solvents. R*OH decay from Figure 9 is displayed on a log−log scale. This highlights the long-time asymptotic behavior (dash−dotted lines, eq 4.15a).

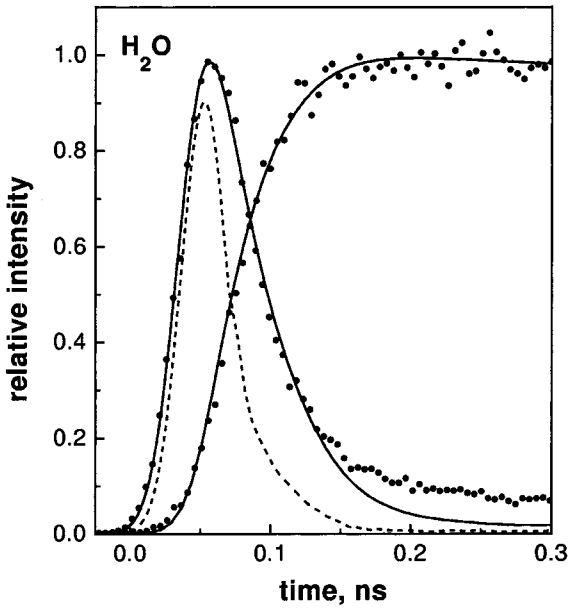

Figure 11. Time-resolved kinetics of 5CN2OH in water. Experimental data (points) are compared with the numerical solution of the DSE (lines) after convolution with the IRF (dashed line). The acid (decaying) and anion (rising) signals represent normalized raw data, which have not been multiplied by $\exp(t/\tau_0')$. The unfitted tail of the acid fluorescence is attributed to 5CN2OH aggregation in water. See section V.B for detail.

We anticipate that ultrafast time-resolved measurements will reveal both HB rearrangement processes suggested from the 5CN2OH steady-state spectra. These solvent conformational changes set the stage for subsequent PTTS, by having the proton already shared between the R*OH chromophore and the HB accepting solvent molecule.

B. PTTS Kinetics. Whereas the HB rearrangements probably occur on subpicosecond time scales, proton dissociation from 5CN2OH takes about 20 ps in water, and considerably longer in the other solvents. Both dissociation and recombination rate parameters, $\kappa_d = k_d$ and $\kappa_r = k_a/(4\pi a^2)$, are determined directly from the time-resolved data by fitting it to the transient solution of eq 4.1; see Figure 9. In all solvents investigated, the kinetics of geminate PTTS appears to be consistent with the mechanism of relative proton−anion diffusion in their mutual electrostatic potential,[23−25,43] once different lifetimes and quenching are taken into account. In all cases, the initial state prepared after photoexcitation is the acid in its relaxed excited state, S_1. It always ejects a proton thermally (in an activated step) to the contact distance, $r = a$, from which the proton may either escape diffusively, recombine adiabatically, or (in protic solvents) quench the excited chromophore to its ground state.

The determination of both forward and reverse rate parameters allows one to estimate pK_a^* and k_{on} directly;[23] see Table 5. The explicit inclusion of quenching suggests that 5CN2OH is by about 0.5 pK units less acidic as compared with an earlier transient study,[14] and nearly 1 unit less acidic than determined by steady-state methods, such as the "Förster cycle".[13] The latter neglects the difference between the Franck−Condon (unrelaxed) and conformationally relaxed excited state, which (judging from our solvatochromic study) is substantial.

The steady-state determination of k_{on} requires high acid concentrations and interpolation to infinite dilution, while the transient geminate data already correspond to the infinite dilution limit. Experience with excited 1,3,5-hydroxypyrenetrisulfonate (HPTS) in water[23] suggests that the transient method yields k_{on}

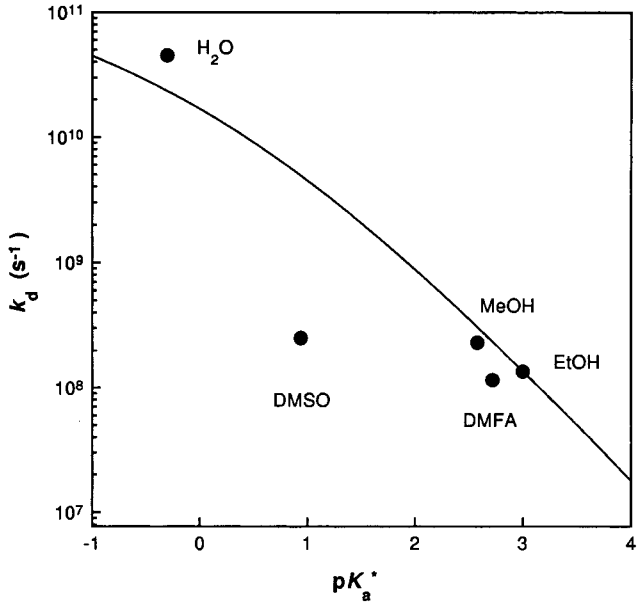

Figure 12. Structure−reactivity correlation for 5-cyano-2-naphthol in various solvents (circles). The line is a fit to eq 7.2 with $k_d^0 = 2.5 \times 10^{11}$ s^{-1} and $\Delta G_0^\dagger = 1.6$ kcal/mol.[19]

values in the diffusion-control limit (ca. 10^{11} M^{-1} s^{-1}) whereas steady-state fluorometric titration values[1] are somewhat smaller (ca. 5×10^{10} M^{-1} s^{-1}). A similar value was also observed for excited 2OH in water.[52] We suggest that for "normal" photoacids, such as HPTS and 2OH, proton recombination is in the diffusion-control limit (in both ground and excited states). However, "super-photoacids" (such as 5CN2OH) dissociate faster and recombine slower in their excited state; hence their k_{on} falls below the diffusion-control limit (Table 5). This trend is in line with structure−reactivity correlations.[30−34]

A more rigorous test for such correlations is provided by k_d, which increases with increasing thermodynamic driving force, $-pK_a^*$, more dramatically than k_{on} decreases. These correlations connect the free energy of activation, $\Delta G^\dagger$, with the free energy of reaction, ΔG, according to

$$\Delta G^\dagger = \Delta G - \Delta G_0^\dagger \ln(n^\dagger)/\ln(2) \qquad (7.2a)$$

$$n^\dagger = [1 + \exp(-\Delta G \ln(2)/\Delta G_0^\dagger)]^{-1} \qquad (7.2b)$$

where the "Brönsted coefficient", $n^\dagger$, is the fractional bond order at the transition state. For $\Delta G = 0$, $n^\dagger = 1/2$ and $\Delta G^\dagger = \Delta G_0^\dagger$. The free energies are related to the rate and equilibrium constants in the usual way

$$K_a^* = \exp(-\Delta G/k_B T) \qquad (7.3a)$$

$$k_d = k_d^0 \exp(-\Delta G^\dagger/k_B T) \qquad (7.3b)$$

These expressions have been applied before to excited-state PTTS reactions.[19,53−55]

Figure 12 compares the rate and equilibria data for 5CN2OH with eq 7.2, using the parameters previously applied to 5CN1OH in methanol/water mixtures:[19] An intrinsic barrier $\Delta G_0^\dagger = 1.6$ kcal/mol, and a maximal dissociation rate coefficient $k_d^0 = 2.5 \times 10^{11}$ s^{-1}. Except for the reaction in DMSO, which deviates from the correlation for an unclear reason, the behavior of the two 5-cyano compounds seems to be quite similar. However, 5CN2OH is considerably less acidic than the 1OH analogue. Hence, even in water it is still quite remote from the "ultimate" limit, $1/k_d^0 = 4$ ps, which may be approached by photoacids with more negative pK_a^* values. This provides one motivation for their synthesis.

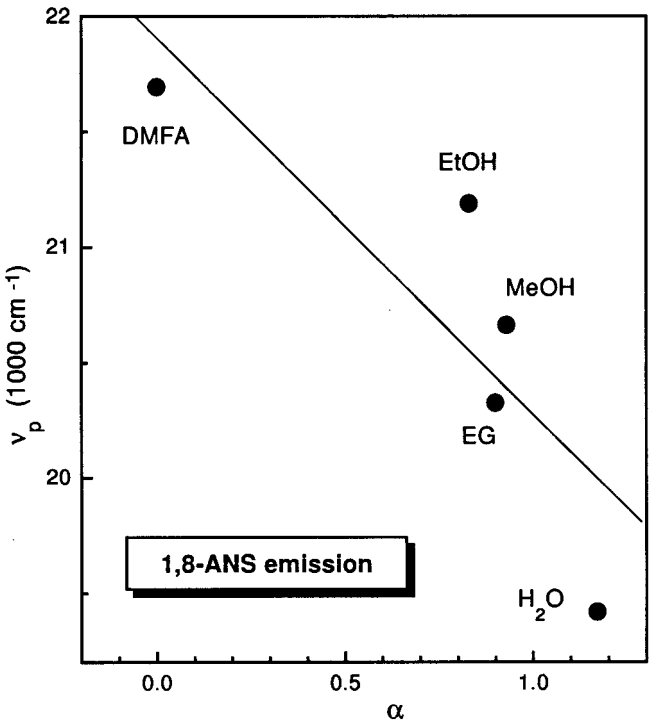

Figure 13. Solvatochromic shifts in the fluorescence emission spectra of 1,8-anilinonaphthalene sulfonate in various solvents.[61] EG = ethylene glycol = ethanediol.

One notes, however, that a time constant of 4 ps is slow as compared with *intramolecular* proton-transfer rates, suggesting that the *intermolecular* rate is controlled by solvent rearrangement. Likewise, proton migration between two water molecules, which takes about 2 ps at room temperature, is thought to require cleavage and formation of two (second-shell) HBs.[56] Somewhat more extensive HB rearrangement may be required to allow proton transfer from an ROH acid to water.

It is also instructive to compare our pK_a^* values, Table 5, with the proton free energy of transfer, ΔG_t, in Table 3. If, as previously suggested,[57,58] proton solvation is the major determinant of photoacid dissociation rates, then 5CN2OH should have been most acidic in DMSO and DMFA, less acidic in water, and least acidic in alcohols. The fact that this is *not* the observed acidity order suggests[43] that anion stabilization plays an important role in determining pK_a^* (hence also k_d) values.

The degree of anion solvation can be inferred from the solvatochromic shifts on the R*O$^-$ band in Figure 4. Water and alcohols induce a considerable hypsochromic (blue) shift. This indicates a better ability to solvate the anion, which more than compensates for their poorer proton solvation ability in comparison with DMFA and DMSO. As seen from Figure 8, anion shifts seem to correlate exclusively with α, the solvent HB donation power. The same trend is observed[48] for the directly excited 2-naphtholate in basic solutions.[59] Due to electron density migration in the excited state from the oxide to the naphthalenic ring, the RO$^-$···HS bond is stronger in the ground electronic state, leading to the observed blue shift for protic solvents.

Blue shifts are not a universal feature of aromatic anions. When the negative group is tethered to a ring site whose electron density *increases* upon excitation, the opposite shift occurs. An example is excited 1,8-anilinonaphthalenesulfonate (1,8-ANS),

in which the charge density is believed to increase at the 8-position.[60] As argued by Sadkowski and Fleming,[61] this results in stronger HBs to the sulfonate anion in the excited state, leading to red shifts for protic solvents. This interpretation is corroborated by Figure 13, which shows that 1,8-ANS emission shifts also correlate with the Kamlet−Taft α scale, but with the opposite trend to that observed here for 2OH derivatives.

In both cases, it is the HB donating ability of the solvent that dictates the extent of anion solvation. Neither data show evidence for a role of polarity (π^*) or dielectric constant (ϵ) in the solvatochromism of the anion. In 5CN2OH (Table 3), MFA (large ϵ) induces a shift just slightly larger than DMFA, whereas methanol (small ϵ) produces a shift almost as large as water. Likewise, in 1,8-ANS (Figure 13), EG and DMFA (similar ϵ) produce different shifts. These observations are apparently at odds with the simple Born solvation model, according to which a unit charge of radius R in a solvent of static dielectric constant ϵ is stabilized energetically by $(2\epsilon R)^{-1}$. Indeed, for ions of different radii in a given solvent (water), a remarkably good correlation with the Born model has been reported.[62] The present investigation of a single ion in *different* solvents reveals a breakdown of the Born model. It may not be surprising if the good correlation with $1/R$ is actually due to an increase of the HB strength with decreasing ionic radii.

The demonstrated importance of HB donation in stabilizing the anion has a mechanistic consequence for excited-state PTTS. Since we have argued that the R*HO···H**S** bond is cleaved upon photoexcitation, we might expect it to re-form simultaneously with the PTTS event. It would be interesting if direct evidence for the formation of the R*O$^-$···H**S** bond could be detected in time-resolved measurements.

Finally, we consider the solvent dependence of the nonradiative and quenching rate parameters for the anion, k_{nr}' and k_q (Tables 3 and 5). Both rate coefficients increase in protic solvents, particularly in water. k_q has been ascribed to geminate contact quenching by the dissociated proton.[21,22] A suggested molecular mechanism for this reaction involves proton attack on the 8 position of the aromatic ring (or on the cyano nitrogen),[13,20] whose electron density is known to increase in the excited state. It appears then that contact quenching is facilitated by a HB pathway to the corresponding ring site. Such an effect is indeed documented for intramolecular proton transfer.[63]

The increase in k_{nr}' in protic solvents was observed also for 1,8-ANS,[61] and attributed to an electron ejection process.[64] Electron ejection was implicated in shortening the excited-state lifetime of other probe molecules.[65] Evidence for the formation of solvated electrons from excited naphtholate and other hydroxyaromatics has been presented.[66−69] While these studies find biphotonic electron ejection on picosecond or subpicosecond time scales, monophotonic electron ejection from the S_1 state of phenol and phenolate has also been reported.[70] Figure 14 shows that this decay process correlates with the Kamlet−Taft α parameter. The strong α dependence for anion solvatochromism in Figure 8, which does not occur for the corresponding acid, suggests hydrogen bonding to the oxide as the origin of this dependence. Thus, if the nonradiative process represents electron ejection, it is facilitated by a HB pathway to the electron-donating group. Consequently, the pathway approach to electron transfer in biological systems[71,72] may be relevant to solution-phase electron transfer as well. The much larger solvent effect on k_q suggests that the pathway concept might be even more important for proton-transfer than for electron-transfer reactions.

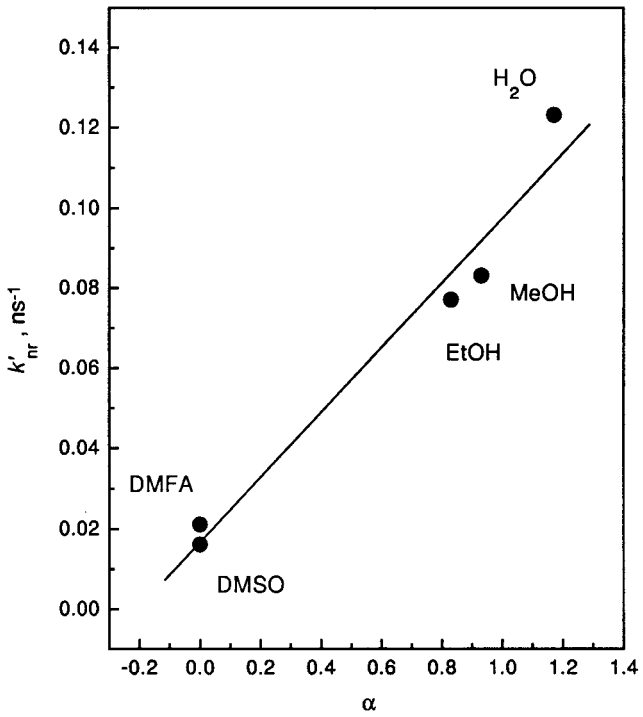

Figure 14. Solvent dependence of the nonradiative decay rate constant of 5-cyano-2-naphtholate generated by excited-state PTTS. Data are from Tables 1 and 3.

Acknowledgment. We thank L. M. Tolbert for a gift of 5CN2OH, M. A. El-Sayed for permission to redo the AQY measurements in his laboratory, and G. W. Robinson for comments on the manuscript. K.M.S. is supported by a postdoctoral fellowship from The Israeli Council of Higher Education. N.A. acknowledges support by The Zevi Hermann Schapira Research Fund. D.H. acknowledges support from the Israel Science Foundation and the James Franck Program for Laser-Matter Interaction. The Fritz Haber Research Center is supported by the Minerva Gesellschaft für die Forschung, mbH, München, FRG.

References and Notes

(1) Weller, A. *Prog. React. Kinet.* **1961**, *1*, 187.
(2) Förster, T. *Pure Appl. Chem.* **1970**, *24*, 443.
(3) Ireland, J. F.; Wyatt, P. A. H. *Adv. Phys. Org. Chem.* **1976**, *12*, 131.
(4) Gutman, M.; Nachliel, E. *Annu. Rev. Phys. Chem.* **1997**, *48*, 329.
(5) Urban, W.; Weller, A. *Ber. Bunsen-Ges. Phys. Chem.* **1963**, *67*, 787.
(6) Demyashkevich, A. B.; Ivanova, L. L.; Kiselevich, V. R.; Kuzmin, M. G. *Sov. J. Chem. Phys.* **1990**, *5*, 759.
(7) Ivanova, L. L.; Demyashkevich, A. B.; Kuzmin, M. G. *High Energy Chem.* **1984**, *18*, 99.
(8) Ivanova, L. L.; Demyashkevich, A. B.; Kuzmin, M. G. *High Energy Chem.* **1985**, *19*, 48.
(9) Kondo, M. *Bull. Chem. Soc. Jpn.* **1976**, *49*, 2679.
(10) Das, R.; Mitra, S.; Mukherjee, S. *J. Photochem. Photobiol. A* **1993**, *76*, 33.
(11) Das, R.; Mitra, S.; Mukherjee, S. *Chem. Phys. Lett.* **1994**, *221*, 368.
(12) Tolbert, L. M.; Haubrich, J. E. *J. Am. Chem. Soc.* **1990**, *112*, 8163.
(13) Tolbert, L. M.; Haubrich, J. E. *J. Am. Chem. Soc.* **1994**, *116*, 10593.
(14) Huppert, D.; Tolbert, L. M.; Linares-Samaniego, S. *J. Phys. Chem. A* **1997**, *101*, 4602.
(15) Solntsev, K. M.; Huppert, D.; Tolbert, L. M.; Agmon, N. *J. Am. Chem. Soc.* **1998**, *120*, 7981.
(16) Kamlet, M. J.; Abboud, J.-L. M.; Abraham, M. H.; Taft, R. W. *J. Org. Chem.* **1983**, *48*, 2877.
(17) Laurence, C.; Nicolet, P.; Dalati, M. T.; Abboud, J.-L. M.; Notario, R. *J. Phys. Chem.* **1994**, *98*, 5807.
(18) Carmeli, I.; Huppert, D.; Tolbert, L. M.; Haubrich, J. E. *Chem. Phys. Lett.* **1996**, *260*, 109.

(19) Pines, E.; Pines, D.; Barak, T.; Magnes, B.-Z.; Tolbert, L. M.; Haubrich, J. E. *Ber. Bunsen-Ges. Phys. Chem.* **1998**, *102*, 511.
(20) Webb, S. P.; Philips, L. A.; Yeh, S. W.; Tolbert, L. M.; Clark, J. H. *J. Phys. Chem.* **1986**, *90*, 5154.
(21) Pines, E.; Fleming, G. R. *Chem. Phys.* **1994**, *183*, 393.
(22) Pines, E.; Tepper, D.; Magnes, B.-Z.; Pines, D.; Barak, T. *Ber. Bunsen-Ges. Phys. Chem.* **1998**, *102*, 504.
(23) Pines, E.; Huppert, D.; Agmon, N. *J. Chem. Phys.* **1988**, *88*, 5620.
(24) Agmon, N.; Pines, E.; Huppert, D. *J. Chem. Phys.* **1988**, *88*, 5631.
(25) Huppert, D.; Pines, E.; Agmon, N. *J. Opt. Soc. Am. B* **1990**, *7*, 1545.
(26) Agmon, N.; Gopich, I. V. *Chem. Phys. Lett.* **1999**, *302*, 399.
(27) Gopich, I. V.; Solntsev, K. M.; Agmon, N. *J. Chem. Phys.* **1999**, 110, 2164.
(28) Agmon, N. *J. Chem. Phys.* **1999**, *110*, 2175.
(29) Gopich, I. V.; Agmon, N. *J. Chem. Phys.* **1999**, *110*, 10433.
(30) Marcus, R. A. *J. Phys. Chem.* **1968**, *72*, 891.
(31) Marcus, R. A. *Faraday Symp. Chem. Soc.* **1975**, *10*, 60.
(32) Agmon, N.; Levine, R. D. *Chem. Phys. Lett.* **1977**, *52*, 197.
(33) Agmon, N.; Levine, R. D. *Isr. J. Chem.* **1980**, *19*, 330.
(34) Agmon, N. *Int. J. Chem. Kinet.* **1981**, *13*, 333.
(35) Birks, J. B. *Photophysics of Aromatic Molecules*; Wiley-Interscience: London, 1970.
(36) Guilbault, G. G. *Practical Fluorescence*; Marcel Dekker: New York, 1973.
(37) Marcus, Y. *Ion Solvation*; Wiley: Chichester, U.K., 1985.
(38) Marcus, Y. *Ion Properties*; Marcel Dekker: New York, 1997.
(39) Krissinel', E. B.; Agmon, N. *J. Comput. Chem.* **1996**, *17*, 1085.
(40) Janz, G. J., Tomkins, R. P. T., Eds. *Non-Aqueous Electrolytes Handbook*; Academic Press: New York, 1972; Vol. 1.
(41) Sharma, L. R.; Kalia, R. K. *J. Chem. Eng. Data* **1977**, 22, 39.
(42) Fillingim, T. G.; Luo, N.; Lee, J.; Robinson, G. W. *J. Phys. Chem.* **1990**, *94*, 6368.
(43) Agmon, N.; Huppert, D.; Masad, A.; Pines, E. *J. Phys. Chem.* **1991**, *95*, 10407. Erratum. *Ibid.* **1992**, *96*, 2020.
(44) Siano, D. B.; Metzler, D. E. *J. Chem. Phys.* **1969**, *51*, 1856.
(45) Agmon, N. *J. Phys. Chem.* **1990**, *94*, 2959.
(46) Mataga, N.; Kubota, T. *Molecular Interactions and Electronic Spectra*; Marcel Dekker: New York, 1970.
(47) Rechthaler, K.; Köhler, G. *Chem. Phys.* **1994**, *189*, 99.
(48) Solntsev, K. M.; Huppert, D.; Agmon, N. *J. Phys. Chem. A* **1998**, *102*, 9599.
(49) Plusquellic, D. F.; Tan, X.-Q.; Pratt, D. W. *J. Chem. Phys.* **1992**, *96*, 8026.
(50) Humphrey, S. J.; Pratt, D. W. *J. Chem. Phys.* **1996**, *104*, 8332.
(51) Chudoba, C.; Nibbering, E. T. J.; Elsaesser, T. *Phys. Rev. Lett.* **1998**, *81*, 3010.
(52) Robinson, G. W.; Thistlethwaite, P. J.; Lee, J. *J. Phys. Chem.* **1986**, *90*, 4224.
(53) Gutman, M.; Nachliel, E. *Biochim. Biophys. Acta* **1990**, *1015*, 391.
(54) Pines, E.; Fleming, G. R. *J. Phys. Chem.* **1991**, *95*, 10448.
(55) Pines, E.; Magnes, B.-Z.; Lang, M. J.; Fleming, G. R. *Chem. Phys. Lett.* **1997**, *281*, 413.
(56) Agmon, N. *Chem. Phys. Lett.* **1995**, *244*, 456.
(57) Lee, J.; Griffin, R. D.; Robinson, G. W. *J. Chem. Phys.* **1985**, *82*, 4920.
(58) Lee, J.; Robinson, G. W.; Webb, S. P.; Philips, L. A.; Clark, J. H. *J. Am. Chem. Soc.* **1986**, *108*, 6538.
(59) Soumillion, J. P.; Vandereecken, P.; Van Der Auweraer, M.; De Schryver, F. C.; Schanck, A. *J. Am. Chem. Soc.* **1989**, *111*, 2217.
(60) Smith, J. C.; Woody, R. W. *J. Phys. Chem.* **1976**, *80*, 1094.
(61) Sadkowski, P. J.; Fleming, G. R. *Chem. Phys.* **1980**, *54*, 79.
(62) Rashin, A. A.; Honig, B. *J. Phys. Chem.* **1985**, *89*, 5588.
(63) Waluk, J. *J. Mol. Liq.* **1995**, *64*, 49.
(64) Fleming, G. R.; Porter, G.; Robbins, R. J.; Synowiec, J. A. *Chem. Phys. Lett.* **1977**, *52*, 228.
(65) Moore, R. A.; Lee, J.; Robinson, G. W. *J. Phys. Chem.* **1985**, *89*, 3648.
(66) Ottolenghi, M. *J. Am. Chem. Soc.* **1963**, *85*, 3557.
(67) Matsuzaki, A.; Kobayashi, T.; Nagakura, S. *J. Phys. Chem.* **1978**, *78*, 1201.
(68) Huppert, D.; Kolodney, E. *Chem. Phys.* **1981**, *63*, 401.
(69) Kotlyar, A. B.; Borovok, N.; Raviv, S.; Zimanyi, L.; Gutman, M. *Photochem. Photobiol.* **1996**, *63*, 448.
(70) Grabner, G.; Köhler, G.; Zechner, J.; Getoff, N. *J. Phys. Chem.* **1980**, *84*, 3000.
(71) Beratan, D. N.; Betts, J. N.; Onuchic, J. N. *Science* **1991**, *252*, 1285.
(72) Skourtis, S. S.; Beratan, D. N. *J. Phys. Chem. B* **1997**, *101*, 1215.
(73) Reichardt, C. *Solvent Effects in Organic Chemistry*; VCH: Weinheim, 1979.